Sol-Gel Synthesized Sorbent Development and Analysis for Column Separations

Lawrence L. Tavlarides
Department of Biomedical and Chemical Engineering
Syracuse University

Outline

The scope of the presentation includes an introduction, synthesis methods of adsorbents, application examined: mercury removal, noble metal separation, and germanium separation, analysis of adsorption in batch and column systems, and conclusions.

Introduction

There are numerous potential uses of adsorbents for gaseous and metal separations in nuclear fuel cycle processing. These include radioactive gas capture (^{85}Kr, ^{129}I and ^{14}C as $^{14}CO_2$) prior to and during dissolution of spent nuclear fuels, technicium separation in the UREX stage of the UREX+1a Process, mercury separation in INEEL/DOE SBR waste and EPA Scrubber solutions, amongst other. The Team at Syracuse University has been engaged in development of new adsorbents for metal ion separations for nuclear, industrial, environmental, and bio-separations.[1-6] These developments employ organic – ceramic synthesis methods to design sorbents at the nano-scale with desirable selectivity, capacity, mechanical properties and stability. We demonstrate the sorbent capabilities through column studies and analysis. This approach can be used for pilot plant column design and studies which can lead to full scale process implementation, and is directly applicable to separations in the nuclear fuel cycle.

- Examples of sorbent separations in the fuel cycle and nuclear waste process:
  - ^{85}Kr, ^{129}I and ^{14}C as $^{14}CO_2$ gas capture from spent fuel dissolution.
  - ^{99}Tc as pertechnetate anion (TcO_4^-) removal from dissolved spent fuel in the UREX process (modified PUREX)
  - Mercury ion separation from nuclear waste solutions.
- New robust sorbents of high selectivity, capacity and stability and stable mechanical properties are required.
- The Team at Syracuse University develops such sorbents using sol-gel methods and demonstrates sorbent usefulness in column applications.

Aqueous Phase Equilibrium of Copper Cyanide Complexes in Cyanide Solutions

The next figure shows why it is important to design a sorbent with the appropriate ligand to match the chemistry of the ions we seek to separate. The figure on the left[1] shows the three different complex forms that copper (I) exists in cyanide solution, such as $Cu(CN)_2^-$, $Cu(CN)_3^{2-}$, and $Cu(CN)_4^{3-}$ depending on the pH and cyanide solution composition. A silica gel immobilized with tetraethylenepenta-amine modified with propyl groups was used to remove copper cyanide from these solutions. The figure on the right[7] shows that the total amount of adsorbed copper cyanide is the sum of the two complexes adsorbed on the surface. Therefore a chelating agent must be selected that can chelate with the metal ion at the expected conditions of extraction. Alternatively, we can alter the solution pH to have favorable binding conditions.

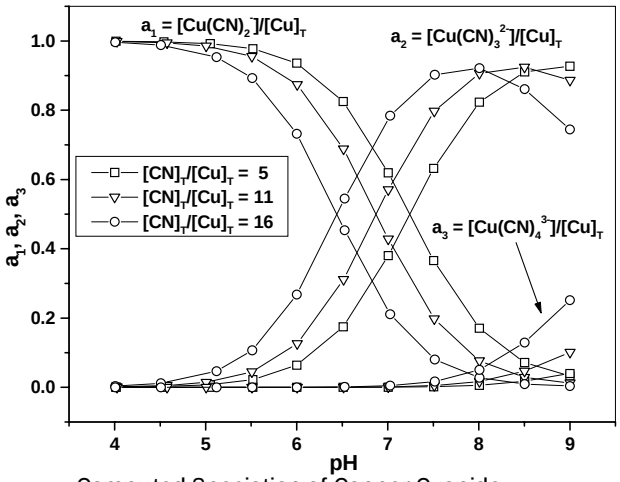

Computed Speciation of Copper Cyanide Complexes in Cyanide Solutions with Respect to the Solution pH (L. L. Tavlarides et al. CRC Press, 2008. With permission)

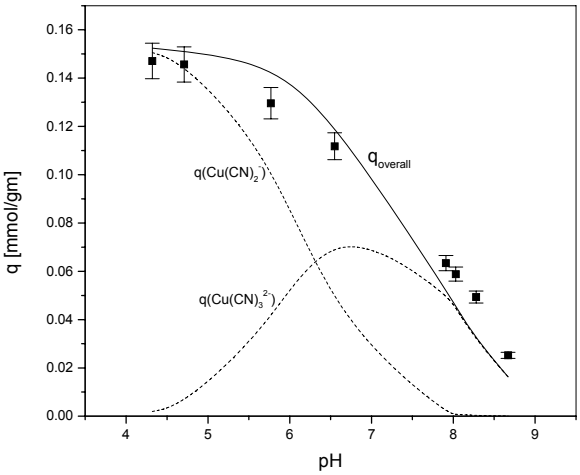

pH Isotherm of Copper Cyanide : [Cu(I)]ini = 200 mg/L; [CN]T/[Cu]T = 16; Experimenal Data, —— : Computed overall copper(I) uptake; – – – – : Computed individual copper(I) complex uptake (J. S. Lee MS Thesis, Syracuse University, 1997.)

Covalent Attachment to Support by Method A

Two basic sorbent network systems are Polymeric Network Systems and Inorganic Network Systems. Polymeric systems have been developed and applied for metal separations from aqueous solutions such as noble metal separations, nuclear waste treatment, and electroplating waste clean-up. Inorganic solid extractants made of functional liqands and inorganic supports attract much attention because of their mechanical strength, thermal stability, wide range of particle size, and well defined pore structure. The latter can be adjusted for rapid intraparticle metal ion diffusion characteristics. We will focus on the inorganic network systems and describe two synthesis approaches. The first involves covalent attachment of the organic ligand to the inorgnanic silica gel by two methods. The first attachment method[1] is shown in this figure. In step 1, a coupling agent (3-chloropropyltrimethoxysilane) is immobilized on the silica gel support. Step 2 attaches the ligand (5-methyl-8-hydroxy-quinoline) by reacting it with the bonded coupling agent.

Step 1: Immobilization of Coupling Agent

Support Surface Coupling Agent

X: Halide, Alkoxy, Acetoxy, and/or Hydroxy
R: Substituted or Unsubstituted Alkyl/Aryl
P: Appropriate Reactive Group

Step 2: Ligand Attachment

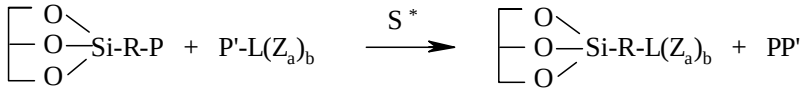

P': Appropriate Reactive Group
Za: Donor Atom of Type 'a'
a = 1 - 8 (upto eight) types
b: Number of each Donor Atom per Ligand
*: Different Reaction Schemes to Attach Ligand

Covalent attachment to support by Method B

The second attachment method[1] is shown on the next figure. In the first step here the functional precursor silane (5-methyl-8-hydroxy-quinoline) and the coupling agent (3-chloropropyltrimethoxysilane) are independently hydrolyzed and condensed. This product is then immobilized on the silica gel.

Step 1: Ligand Attachment to Coupling Agent

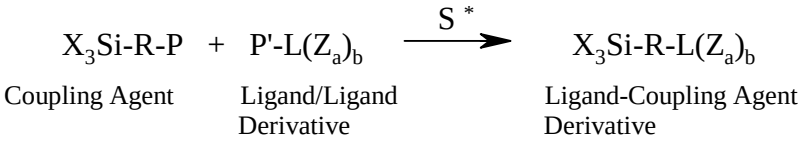

*: Different Reaction Schemes to Attach Ligand

Step 2: Immobilization of Ligand Coupling Agent Derivative

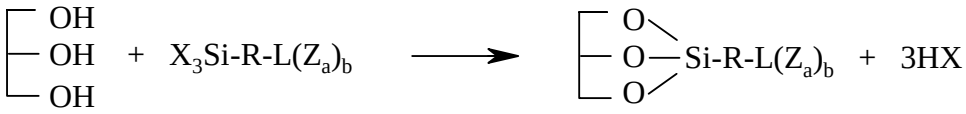

Choice of Ligand Attachment Scheme:

1. **Depends on Reactive Groups and Conditions**
2. **Desire to Achieve Ligand with Specific Donor Atoms and Preferred Geometry**
3. **Desire to Achieve High Ligand Density on the Support Surface**

Adsorbent Prepared by Covalent Bonding Using Silane-coupling Agent

The resulting structure by either method is shown on the following slide. The functional portion of the attached ligand is free in the silica pores to complex the metal ion.

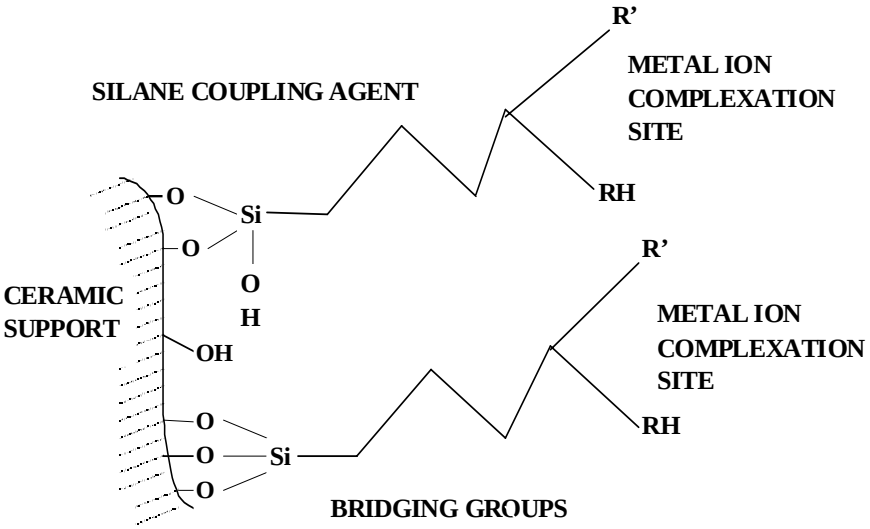

Examples of Adsorbents Developed by Covalent Attachment Technique

The next figure shows adsorbents developed by the covalent attachment technique using either or both methods described in the previous sections. These sorbents are applied to a variety of metal ion separations as shown.[2]

Support	Functional Group	Method/Coupling Agent	Metal Ions
Silica gel	5-methyl-8-hydroxy-quinoline	Organic functional silane derivatives in solutions and surface	Pb(II), Cu(II), Ni(II), Cd(II)
Silica gel	Thio Sulfide acid	Organic functional silane in solution	Cd(II), Hg(II), Zn(II), Pb(II)
Silica gel	Primary secondary and tertiary amines, and diazole	Organic functional silane on surface	Cu(II), Ni(II), anionic cyanide complexes, $Cr_2O_7^{2-}$, CrO_4^{2-}
Silica gel	Pyrogallol	Derivatization on surface modified with organo-functional silane	Antimony(III) Al(III), Cu(II)

Recent Work on Organo-ceramic Adsorbents

A second approach to synthesis of organo-ceramic adsorbents led to a series of adsorbents called SOL-AD.[3,5] In this approach a functional precursor is co-condensed with a hydrolyzed cross-linking agent. Advantages of these materials are high ligand densities, homogeneous distributions of the functional moiety throughout the matrix, and controlled pore characteristics.

As an example the functional precursor containing an active group, such as 3-mercapto-propyltrimethoxysilane is hydrolyzed and undergoes self-condensation. Likewise, a cross-linking agent, such as tetra-ethoxy silane is hydrolyzed and undergoes self-condensation. The two reaction systems can be combined at a certain time to maximize the density of ligand in the matrix and properties of the matrix.

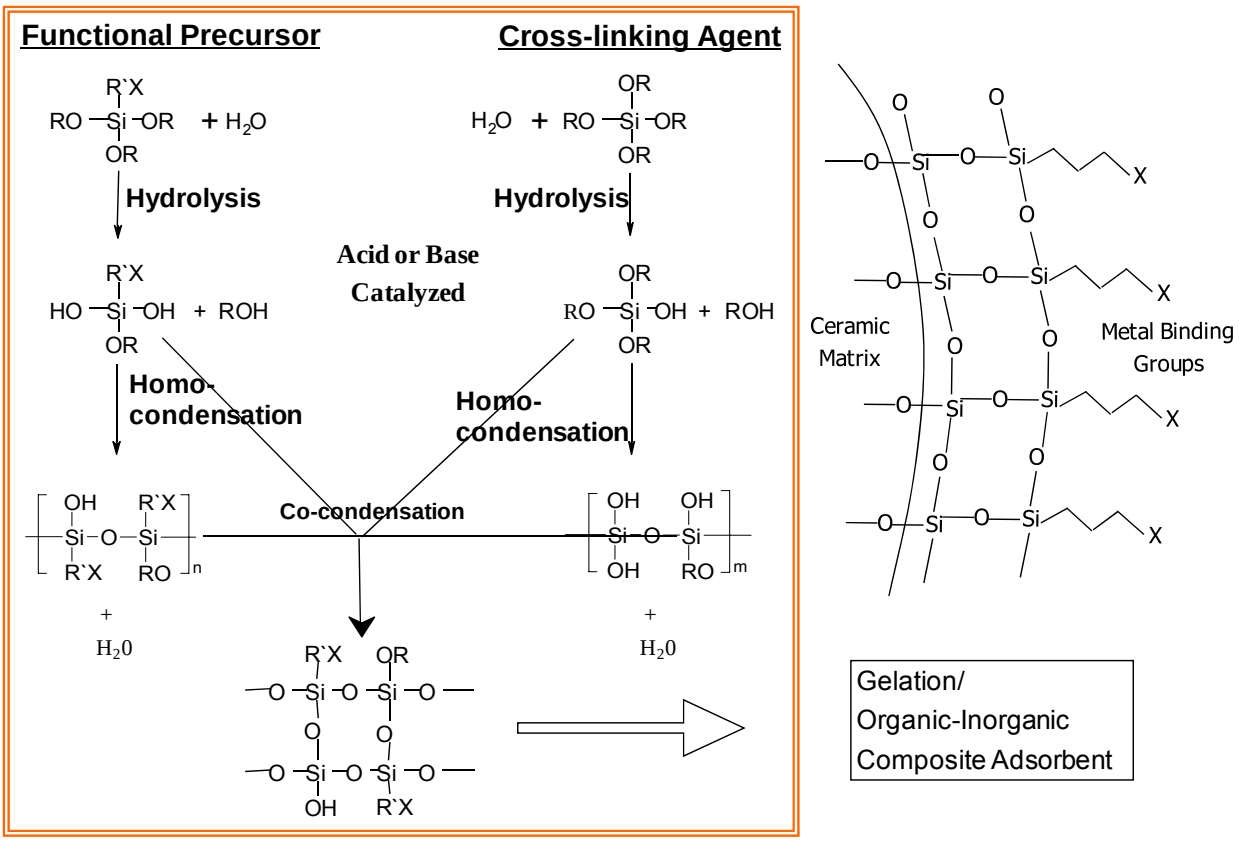

Functional Group Clustering

The evolution of the polymers of the hydrolysis-condensation reaction of the precursor, 3-mercaptopropyltrimethoxysilane (MPS) is shown via the ^{29}Si-NMR spectra on this figure.[3] Oligomers composed mostly of the T2 silicons are the most favorable for the formation of functional clusters.

^{29}Si-NMR Spectra: Oligomerization vs. time
3-mercaptopropyl-trimethoxysilane (MPS)

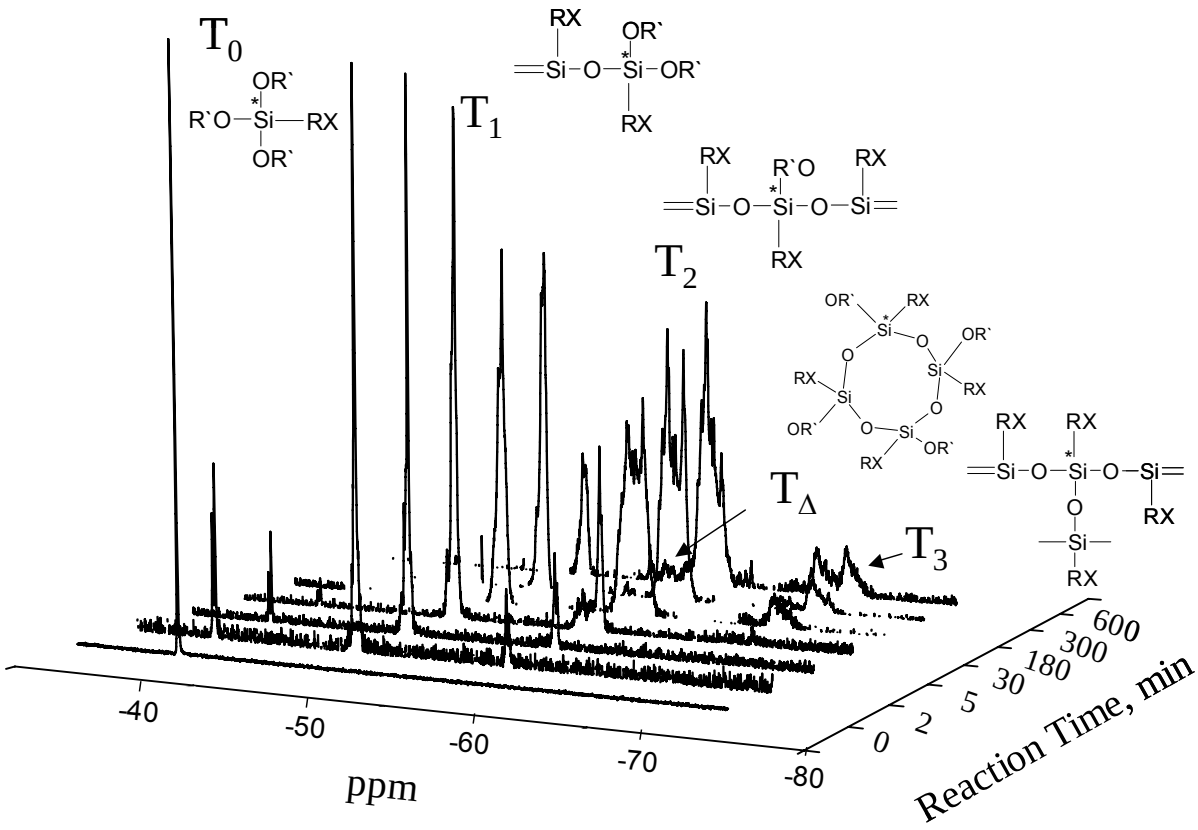

Oligomerization of MPS and Cd(II) Uptake Capacity

This figure[3] shows that the uptake capacity of Cd (II) is maximized when the MPS oligomerization reaction time is chosen to maximize the concentration of the T2 oligomer.

SOL-AD-IV: Thiol Functionalized Adsorbent

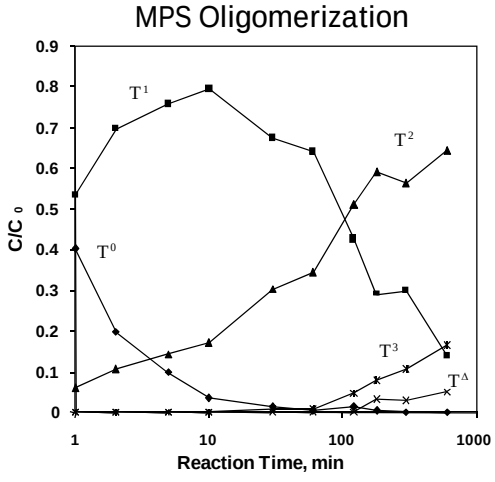

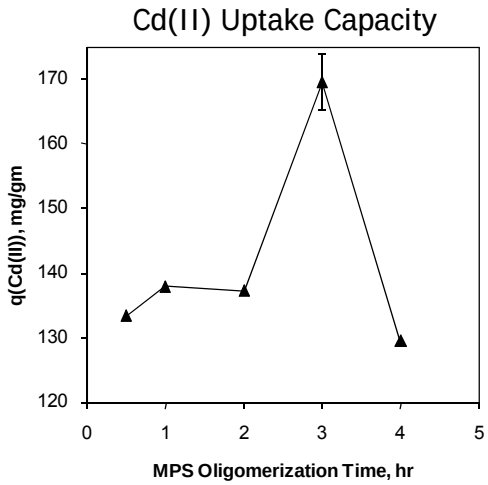

Importance of Molar Ratio to Adsorbent Properties

This next figure shows the importance of the ratio of the CS/FPS on adsorbent.[3]
Here q_a and q_t are the actual capacity and theoretical capacity of SOL-AD-IV with the molar ratio of CS to FPS. For a q_a ratio less than 2 we see that the actual capacity decreases below the theoretical capacity due to (a) poor pore accessibility, (b) strong hydrophobicity, and (c) poor structural integrity. Also, Dp increases and SA decreases. As the CS to FPS ratio increases above 2, q_a follows the theoretical capacity, and the SA increases while the pore diameter stabilizes to a constant value as a greater portion of the pores are made up with the CS.

SOL-AD-IV

q_a decreases:

- poor pore accessibility
- strong hydrophobicity
- poor structural integrity

Dp increases and SA decreases:

- coagulation and entanglement of precursor oligomers

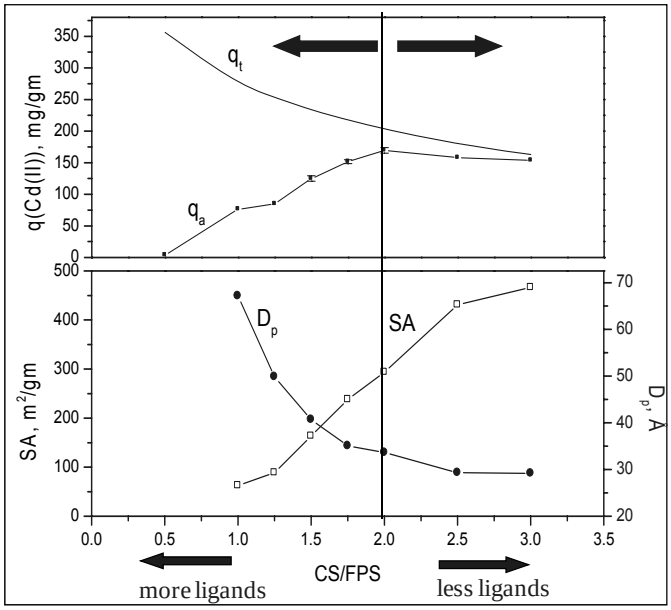

q_a follows :

- theoretical capacity

SA increases and Dp stays constant

- greater portion of pores made up with CS

Adsorbents Developed by Sol-Gel Processing

The next figures show some of the adsorbents we developed by sol-gel processing. They include (a) Thiol system (SOL-AD-IV)[3,5], (b) Imidazole system (SOL-IPS)[8,9], (c) Kelex-100 system (SOL-KELEX)[10], and (d) Pyrazole System (SOL-PzPs)[6].

- Thiol System (SOL-AD-IV)
  - Precursor : 3-(mercaptopropyl)-trimethoxysilane
  - Target Ions: Cadmium, Lead, Mercury, and Copper

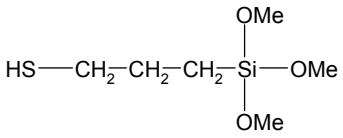

- Imidazole System (SOL-IPS)
  - Precursor : 1-(triethoxysilylpropyl)-imidazoline
  - Target Ions: Platinum, Palladium, Gold, and Rhodium

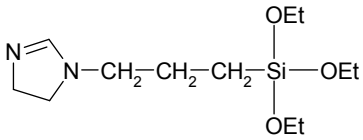

Synthesis Conditions of Sol-Gel Adsorbents

These figures show the conditions of the synthesis reactions to produce the four sol-gel adsorbents shown on the previous four figures. Note how the FPS and CS condensation time vary for each sorbent.[3, 5, 6, 8-10]

SOL-AD-IV
- Chemical Compositions
  - MPS : TEOS = 1 : 2
  - MPS : EtOH : H_2O : HCl : NaCl = 1 : 3 : 3 : 0.01 : 0.01
  - TEOS : EtOH : H_2O : HCl : NaCl = 1 : 4 : 4 : 0.006 : 0.01
- Reaction Time
  - MPS condensation : 3 hrs
  - TEOS condensation : 30 mins
  - Co-condensation : 5 mins

SOL-PzPs-BD-5
- Chemical Compositions
  - PzPs : TEOS = 1 : 2
  - PzPs : EtOH : H_2O : HCl : NaF = 1 : 3 : 3 : 0.01 : 0.01
  - TEOS : EtOH : H_2O : HCl : NaF = 1 : 4 : 4 : 0.01 : 0.01
- Reaction Time
  - PzPs condensation : 2 hrs
  - TEOS condensation : 15 mins
  - Co-condensation : 5 mins

SOL-KELEX
- Chemical Compositions
  - APS : TEOS = 1 : 3
  - APS : EtOH : H_2O : HCl = 1 : 4 : 1 : 10^{-5}
  - TEOS : EtOH : H_2O : HCl = 1 : 3 : 1 : $3x10^{-5}$
- Reaction Time
  - MPS condensation : 15 mins
  - TEOS condensation : 15 mins
  - Co-condensation : 5 mins

SOL-IPS
- Chemical Compositions
  - IPS : TEOS = 1 : 2
  - IPS : EtOH : H_2O : HCl = 1 : 3 : 2 : $4.5x10^{-3}$
  - TEOS : EtOH : H_2O : NaF = 1 : 4 : 1 : $0.67x10^{-3}$
- Reaction Time
  - IPS condensation : 30 mins
  - TEOS condensation : 30 mins
  - Co-condensation : 5 mins

Comparison of Sol-Gel Adsorbents with Other Types of Adsorbents

These figures compare the sol-gel adsorbents we prepared with others available in the literature.[2, 4, 12-19] For example; our SOL-AD-IV sorbent has a greater capacity for mercury than available sorbents. In most comparisons the sol-gel sorbents have a greater capacity.

Palladium Separation

Adsorbent	Capacity	BET Analysis		Functional Group	Reference
		D (Å)	SA (m^2/g)		
Chelating resin	65.4			DEHTPA / impregnated polymer resin	Rovira et al., Sol. Extr. & Ion Exch., 17, 1999
Doulite Ge-73 resin	28.5			Thiol / polymer resin	Iglesias, Anal. Chim. Acta, 381, 1999
SOL-IPS	162.3			Imidazole/ sol-gel processing	This study
SOL-PzPs	150.8	37	437	Pyrazole / sol-gel processing	This study

Mercury Separation

Chelating resin	562	107	41	Thiazole and thiazolin / polymer resin	Sugii A. et. al., Talanta. 27, 1998
Functionalized silica	505	55	900	Thiol / covalent attachment on SAMMS	Feng X. et. al., Science, 276, 1997
SOL-AD-IV	1280	82	640	Thiol / sol-gel processing	This study

Germanium Separation

Adsorbent	Capacity	BET Analysis		Functional Group	Reference
		D (Å)	SA (m^2/g)		
Activated Carbon	10.1			$H_3PO_4^-$ activated carbon,	J.P. Marco-Lozar
Cellulose	115.2			di(2-hydroxyethyl)amine / polymer	Y. Inukai
Goethite	4.3			$FeSO_4$ / oxidative hydrolysis	O.S. Pokrovsky
SOL-KELEX	23.8	72	421	Kelex-100 / sol-gel processing	This study

Cadmium Separation

ISPE-302	19.7			Cyanex-302 / solvent deposion on silica	Deorkar et al., Emerging Separation Technology II, 1996
ICAA-S	71.1			Thiol / covalent bond on silica	Deorkar et al., Ind. Eng. Chem. Res., 36, 1997
Chelating resin	146.0			Mercaptoacetamide / polymer resin	Colella et. al., Anal. Chem., 52, 1980
SOL-AD-IV	222.3	82	640	Thiol / sol-gel processing	This study

Applications Studied

We now turn to several applications of these sol-gel materials to important metal ion separation processes. We will outline our results for (a) mercury removal including Scubber solution and DOE acidic nuclear waste solutions, (b) noble metal separation, and (c) germanium separation.

SOL-AD-IV for Mercury Separations

The mercury separation problem was motivated by the presence of mercury in INEEL/DOE sodium bearing waste solutions and in EPA scrubber solutions and the need for separation. This chart shows the composition of these solutions. The EPA scrubber solution shown is used in these studies except that mercury concentrations are adjusted as needed.

Species	Compositions (molar)	
	INEEL/DOE SBW Solution	EPA Scrubber Solution
Al^{3+}	0.6	-
Ca^{2+}	-	0.00873
Cl^{-}	-	0.03102
F^{-}	0.1	-
K^{+}	0.18	-
H^{+}	***2***	***pH 5***
Hg^{2+}	***0.00758* (1500ppm)**	***$2.5x10^{-6}$* (0.5ppm)**
Mg^{2+}	-	0.00206
Na^{+}	-	0.03104
NH_4^{+}	-	0.01144
NO_3^{-}	3.8	0.02158
SO_4^{2-}	-	0.00572
Zn^{2+}	-	0.00046

Equilibrium Isotherms

Equilibrium isotherms are used to show the uptake capacity of adsorbents over a range of pH values and concentration of the solute in solution. The adsorption equilibrium behavior of SOL-AD-IV shown on this slide shows a high mercury uptake capacity of ~510mg/g at 0.5mg Hg/L, which is the scrubber water concentration.[5] Capacities as high as ~750-800 mg/g are obtained at 200 mg/L solution concentrations. We also developed a two species equilibrium model when acetate ion is present in the system. In this case, mercury chloride complexes with the ligand in reaction 1 and mercury acetate complexes with the ligand in reaction 2. The equilibrium model is shown below. When no acetate is present the model reduces to a simpler form. This model was used to predict the isotherms.

EPA Scrubber Matrix Solution

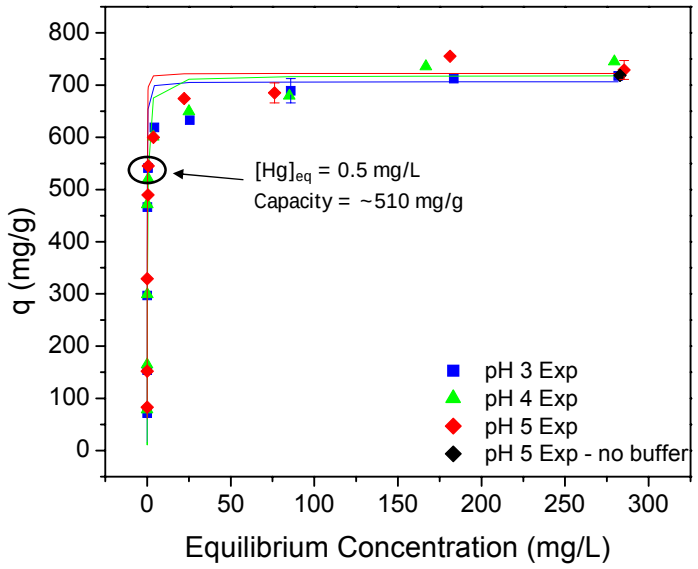

Batch Contactor Mode

Adsorbent: 0.2g of SOL-AD-IV
Solution:
100 ml of simulated solution
Total Mercury = 300 – 1800 mg/L
Buffered = 0.2M Sodium Acetate
Contact time: 24 hrs

$$\overline{RSH} + HgCl_2 \overset{1}{\Leftrightarrow} \overline{RS \cdot HgCl} + H^+ + Cl^-$$

$$\overline{RSH} + HgAc_4^{-2} \overset{2}{\Leftrightarrow} \overline{RS \cdot HgAc} + H^+ + 3Ac^-$$

$$q = \frac{S_T K'_{eq1}[HgCl_2] + S_T K'_{eq2}[HgAc_4^{-2}]}{1 + K'_{eq1}[HgCl_2] + K'_{eq2}[HgAc_4^{-2}]}$$

Breakthrough Curve Study

To evaluate the performance of the adsorbent we did column studies to determine the breakthrough curve and provide a check on the uptake capacity. The results of these experiments are shown on this slide. The figure on the left shows little breakthrough up to 5500 bed volumes of flow.[5] At bed saturation the column capacity was 391mg/g. Further, the effluent concentration is less than 1ppb up to approximately 5000 bed volumes.

EPA Scrubber Matrix Solution

Column: 0.7 cm ID
SOL-AD-IV = 0.175 g
Solution: Simulated scrubber solution
C_0 = 0.564 mg/L, pH = 5.0

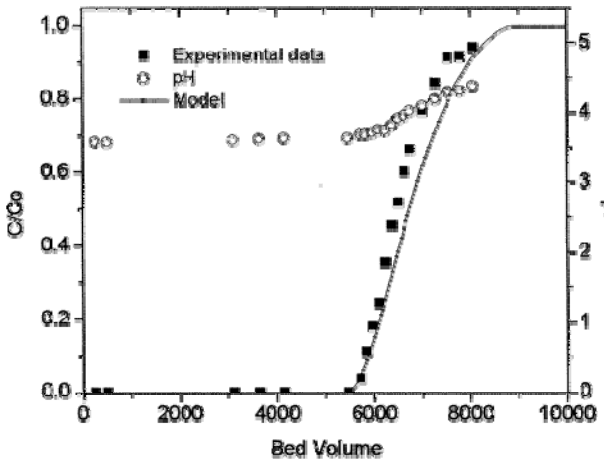

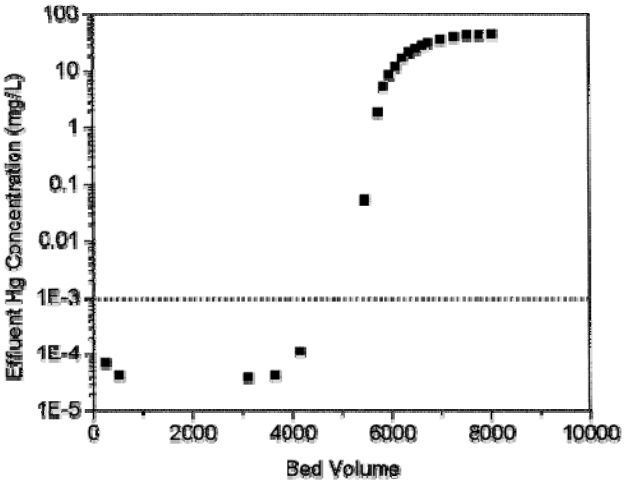

Flow rate: 6 ml/min

Stability of SOL-AD-IV for Multiple Adsorption/Desorption Cycles

An important factor is the operational stability of sorbents after multiple adsorption/desorption cycles. This slide shows such behavior of SOL-AD-IV. The conditions of the experiments are shown on the right of the slide. Here q_i is the mercury uptake after the ith cycle and q_o is the uptake capacity after the first cycle. The adsorption capacity gradually decreases through the 10 th cycle and then retains approximately 90% of the original capacity through 25 cycles.[5] This thiol adsorbent is chemically stable in 12 M HCl stripping solutions.

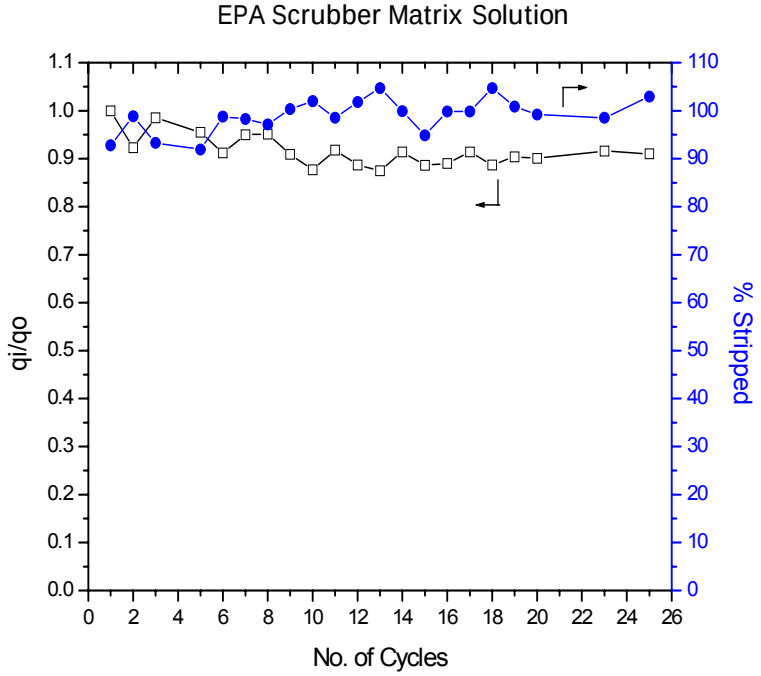

Column Operation Mode

m = 0.2g SOL-AD-IV
Flow rate = 0.8ml/min
Loading:
1 Liter of 300mg/L Hg @ pH 5
Stripping:
25ml of 12.1M HCl
Washing:
10ml of DI water before and after stripping

q_0 = 760 mg/g
Capacity loss after 25 cycles = ~ 10%

Noble Metal Separation

The second adsorption system we will evaluate is SOL-PzPs (the pyrazole functional adsorbent) which we demonstrate can separate noble metals of palladium, platinum and gold.[6] The chemistry of adsorption is shown here.

- SOL-PzPs: Pyrazole Functionalized Adsorbent
- Extraction and Separation of Pd(II), Pt(IV), and Au(III) from 2.0 M HCl Solutions

• Protonation of Functional Ligand $H^+ + \overline{R} \Leftrightarrow \overline{RH^+}$

• Adsorption of Chlorocomplexes $M^{X-} + X\,\overline{RH^+} \Leftrightarrow \overline{M(HR)_X}$

M^{X-} is $PdCl_4^{2-}$, $PtCl_6^{2-}$, and $AuCl_4^-$

$\overline{R}$ is Functional Ligand

$\overline{RH^+}$ is Protonated Ligand

Adsorption Isotherm

The adsorption isotherms were constructed as mentioned previously and we see that the palladium isotherm is the Langmuir form. Further in the practical range of concentration of <0.2 mmol/L, complete palladium separation from platinum and gold can be achieved.[6]

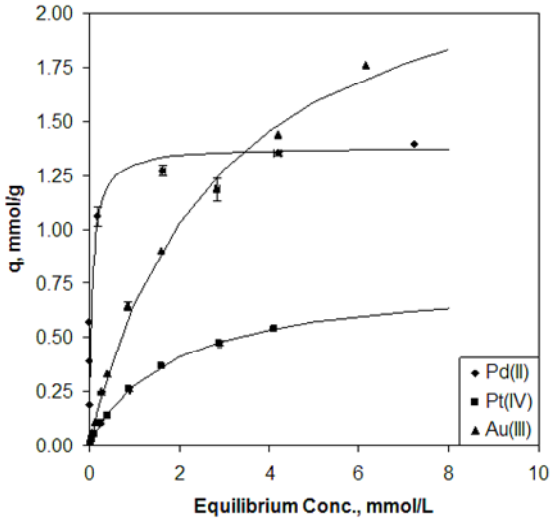

- Affinity order:
- Pd(II) >> Au(III) > Pt(IV)
- In practical conc. Range (<0.2 mmol/L):
  Complete Pd(II) separation

$$q_{PdCl_4^{2-}} = \frac{q_m K[PdCl_4^{2-}]}{1 + K[PdCl_4^{2-}]}$$

q_m = 1.284 mmol/g
K = 182 L/mmol

Breakthrough in Packed Column

Again we have to test the adsorbent in column operation with a typical feed composition one expects from noble metal leachate solutions. The figure on the left shows that copper and iron do not adsorb and that the platinum and gold are effectively displaced by palladium due to competitive adsorption. Appropriate stripping solutions are evaluated and thiourea solution in HCl removes 100% of the Pd and 91% of the Au from the solution.[6]

- Mixed Metal Feed Solution

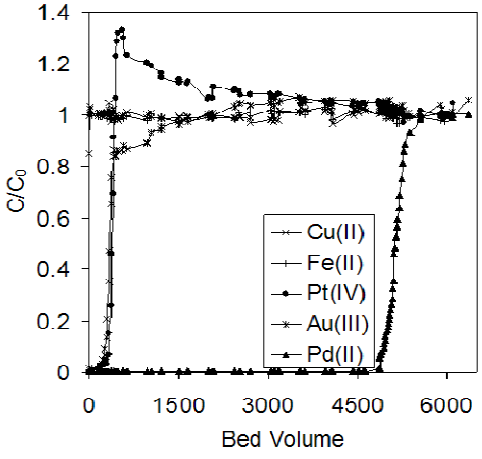

- Feed Solution
  - 0.1 mmol/L each of Pd, Pt, and Au
  - 2.5 mmol/L each of Cu(II) and Fe(II)
- Column Bed Volume = 2.98 ml

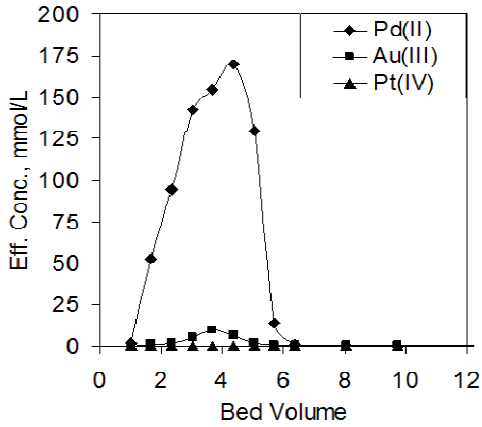

- 0.5 mol/L thiourea in 0.1 mol/L HCl
- Stripping Efficiency (Pd : 100 %, Au : 91 %)
- 12 liters into 0.021 liters

Adsorption Mechanism and Isotherm

The third system we present in that for germanium separation from zinc leachate ores. This system is interesting because of the high value of germanium due to the use in semi conductors. ($ 1700/ kg) The adsorption isotherms here show a Langmuir type behavior, although the detailed chemistry gives the complicated isotherm model shown on the right.[10] We note that at the pH range studied essentially only $Ge(OH)_4$ is present.

- Adsorption Mechanism (SOL-KELEX)

$$Ge(OH)_4 + 2\overline{HR} \leftrightarrow \overline{GeR_2(OH)_2} + 2H_2O \qquad q = \frac{4K_{eq}[Ge(OH)_4][\overline{HR}]_T{}^2}{(1+\sqrt{1+8K_{eq}[Ge(OH)_4][\overline{HR}]_T})^2}$$

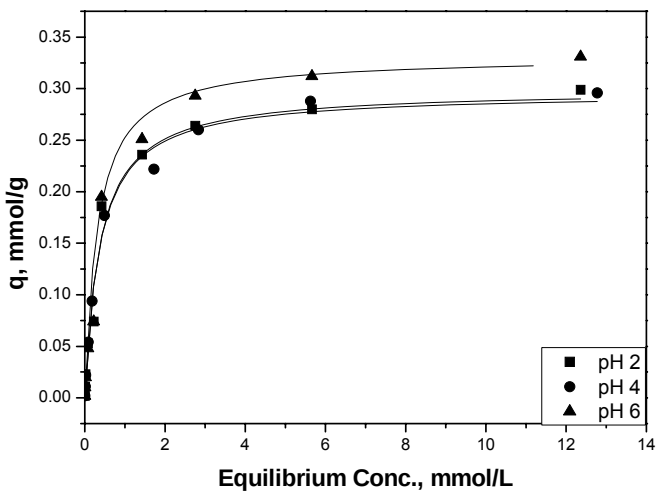

- ini Conc. = 1 ~ 1000ppm
- pHe = 2, 4, 6
- Adsorbent = 0.1 g
- Solution volume = 15 ml
- Batch Exp for 24hrs
- Buffer = 0.05M NaAc
- q_{max} = 21.5mg/g
- (0.33mmol/g)
- K_{eq} (L/mmol^2) = 2.65

Column selectivity (17 metals)

A major problem with germanium separation from zinc leachate solutions is the presence of numerous metals. Accordingly a selective ligand is required to yield a relatively pure germanium product. This figure shows the selectivity of SOL-KELEX for germanium in a column extraction from a simulated leachate solution. Germanium has the lowest concentration. The selectivity is about 91% germanium, 4% tin, and 5% combined of the four other metals shown.[10] Thus, multiple column adsorption/ stripping would yield an acceptable product.

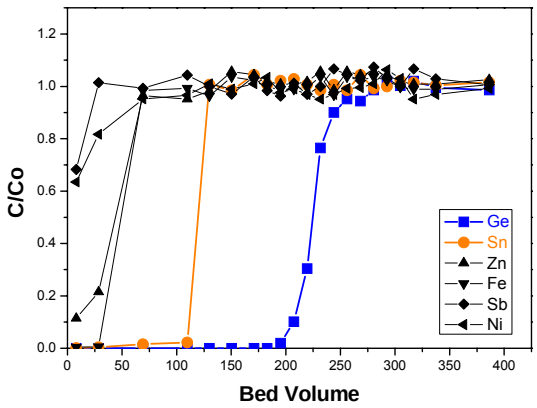

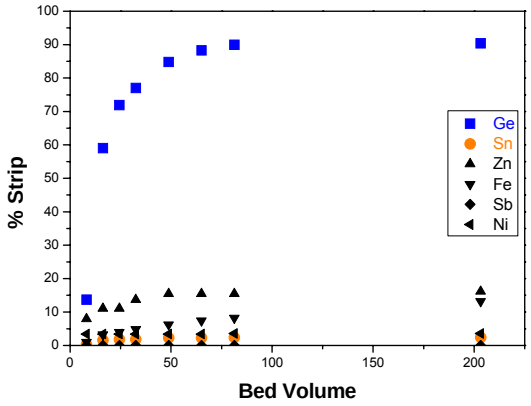

Simulated solution composition

- **Zn: 2.28 ppm**
- **Ni: 2.08 ppm**
- **Fe: 2.21 ppm**
- **Sb: 1.39 ppm**
- **Sn: 1.37 ppm**
- **Ge: 0.59 ppm**
- As: 0.59 ppm
- Mg: 1.97 ppm
- Cu: 1.98 ppm
- Ca: 2.21 ppm
- Na: 1.28 ppm
- Pb: 2.41 ppm
- Al: 2.65 ppm
- Co: 2.23 ppm
- Cd: 2.04 ppm
- Mn: 1.34 ppm
- In: 2.06 ppm

Modeling of $HgAc_4^{2-}$ Adsorption Kinetics in Batch and Packed Column

It is necessary to develop models to describe the adsorption kinetics of the systems and permit analysis of fixed bed columns. These models can then be employed to design adsorption columns and process analysis can be executed. To outline the method, we will describe two laboratory experimental equipment, the analysis employed and results obtained for the SOL-AD-IV (thiol) adsorbent used in mercury separations. The equipment used are shown in this slide.

For the batch differential recycle reactor (BDRR), feed solution is circulated by a pump from a reservoir to a differential reactor containing a layer of the adsorbent between glass beads. A sample of the reservoir solution is taken at time intervals for mercury concentration analysis. The conditions are specified.

For the packed column the adsorbent is placed in the column of the geometry specified and flow of the mercury solution is started. Samples are taken at time intervals from the column exit flow and analyzed for mercury concentration. The conditions are specified. Different particle size ranges can be used but the 125-180 um range provides rapid adsorption with acceptable pressure drop.

Batch Differential Recycle Reactor

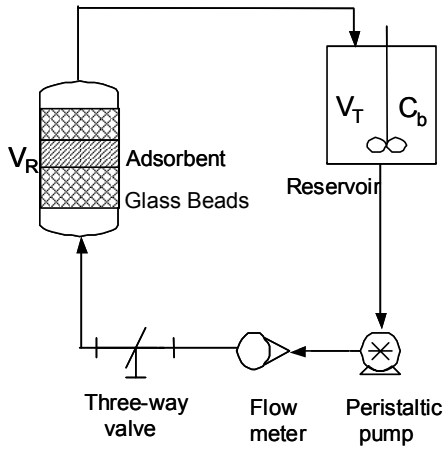

SOL-AD-IV (Thiol) = 0.2 gm (125 – 180 μm)
1.0 cm ID column
Vol. of solution = ~ 500 ml
Flow rate = ~ 40 ml/min

Packed Column

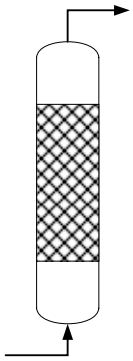

SOL-AD-IV (Thiol) = 2.0 gm (125 – 180 μm)
0.7 cm ID column
Solution = 0.5-50mg/L Hg, pH 5, 0.1M Ac
Flow rate = ~1.0 ml/min

Mass Transfer in Adsorption Processes

The details of mass transfer in adsorption processes are described in this slide.[11] For interpellet / intrapellet mass transfer the solute can undergo the three steps described. These include interphase mass transfer (2), intrapellet mass transfer by pore diffusion or/and surface diffusion (3a, b), and surface adsorption (4). In fixed beds the solute flows down (up) through the bed due to convection motion and can undergo axial dispersion (1a) and radial dispersion (1b).

a. Fixed Beds
b. Intrapellet mass transfer

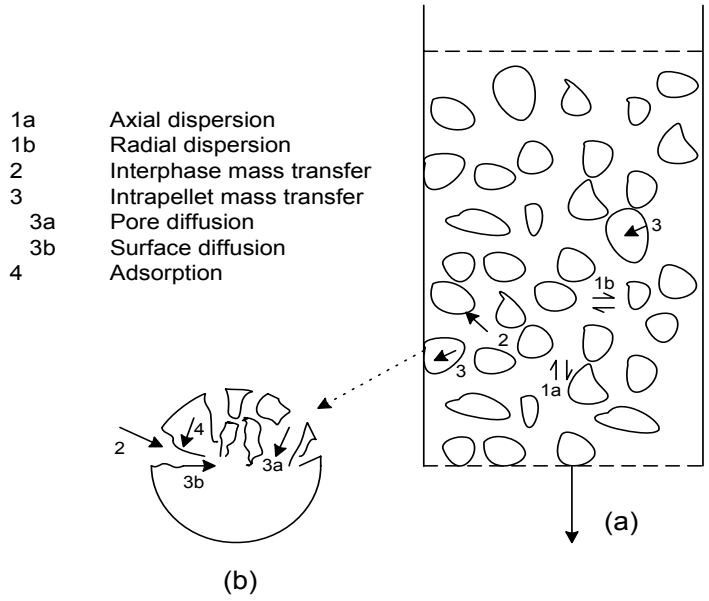

Kinetic Modeling of Adsorption

There are several approaches to model the adsorption of solutes in particles. The first of two we have employed assumes that the kinetics of surface adsorption controls; the chemical reaction model. This case is likely for small particle size ranges where intrapellet diffusional resistances are small and high flow rates are employed through the bed.

For mercury adsorption on SOL-AD-IV, the adsorption stoichiometric equation, the corresponding rate expression, the design equation for the BDRR and the solution is presented. A statistical method is employed to obtain the best value for the forward reaction rate coefficient k_2 and the reverse coefficient is obtained from $K_{eq,2}$. The model can be used to describe adsorption kinetics.

- Case 1: Chemical Reaction Model: Kinetics of Surface Adsorption Controls. Hg adsorption on SOL-AD-IV (pH ≥ 5; acetate buffered chloride solution):

$$\overline{RSH} + HgAc_4^{2-} \underset{k_{-2}}{\overset{k_2}{\leftrightarrow}} \overline{RS \cdot HgAc} + H^+ + 3Ac^- \qquad K_{eq} = k_2 / k_{-2}$$

$$rate = -\frac{d[HgAc_4^{2-}]}{dt} = k_2[\overline{RSH}][HgAc_4^{2-}] - k_{-2}[\overline{RS \cdot HgAc}][H^+]\{Ac^-\}^3$$

Design Equation for Batch Differential Recycle Reactor:

$$-rate = \left(\frac{V_R + V_T}{V_R}\right)\frac{dC_T}{dt}$$

Solving above two equations (linear regression method of Levenberg-Marquardt)

$$C(t) = \frac{De^{Ak_2} - EB}{2B - 2e^{Ak_2}} \qquad A,B,D,E = \text{constants} = f(C_{B0}, S_T, M, V, [H^+].\{Ac^-\})$$

Solve for k_2 : k_{-2} obtained from $K_{eq,2}$

The second approach employed is when we assume that the rate of adsorption is controlled by solute transport through the film and particle pores. The chemical rate of adsorption is assumed instantaneous. This case is likely for larger particle size ranges and small pore diameters.
A macroscopic balance is made for the BDRR where the average mass of mercury adsorbed per unit mass of adsorbent, q, is calculated for average particle size with appropriate initial and boundary conditions.

The pore diffusion equations are solved to calculate the rate of mercury acetate adsorbed into an average particle with time during the BDRR experiment. These equations can also be employed to describe adsorption kinetics.

- Case 2: Film-Pore Model: Solute Transport Through Film and Pore Adsorption Controls (Spherical Particle):

Macroscopic Balance for Batch Differential Reactor:

$$V\,(C_{b_o} - C_b) = M\,\bar{q}$$

$$\bar{q} = \frac{3}{R_p^3}\int_0^R q\, r^2 dr$$

$$q = [\overline{RS \cdot Hg \cdot Ac}] = \frac{S_T K_{eq2}[HgAc_4^{2-}]}{[H^+][Ac^-]^3 \gamma_{Ac}^3 + K_{eq2}[HgAc_4^{2-}]}$$

Pore Diffusion Equation:

$$\left[\varepsilon_p + \rho_p \frac{\partial q}{\partial c}\right]\frac{\partial c}{\partial t} = \frac{D_p}{r^2}\frac{\partial}{\partial r}\left(r^2 \frac{\partial c}{\partial r}\right)$$

$$c = 0, \qquad t \le 0 \qquad 0 \le r \le R$$

$$\frac{\partial c}{\partial r} = 0, \qquad r = 0$$

$$D_p \frac{\partial c}{\partial r} = k_f\,(c_b - c), \qquad r = R$$

The last set of equations we will discuss are those used to model the performance of the adsorption column. These are shown on the next figure and include the column mass balance and the same set of pore diffusion equations for intraparticle mass transfer we used in previous slide.

- Modeling Column Adsorption (Film-Pore Resistance Controls Adsorption)

Column Mass Balance

$$u_s \frac{\partial c_b}{\partial z} + \varepsilon \frac{\partial c_b}{\partial \theta} + \rho_b \frac{\partial \overline{q}}{\partial \theta} = 0$$

$$c_b = 0, \qquad z \ge 0 \quad and \quad t \le 0$$

$$c_b = c_{b0}, \qquad z = 0 \quad and \quad t > 0$$

where

$$\rho_b = (1-\varepsilon_b)\rho_p, \ \theta = t - z\varepsilon / u_s$$

Pore Diffusion Equation:

$$\left[\varepsilon_p + \rho_p \frac{\partial q}{\partial c}\right]\frac{\partial c}{\partial t} = \frac{D_p}{r^2}\frac{\partial}{\partial r}\left(r^2 \frac{\partial c}{\partial r}\right)$$

$$c = 0, \qquad t \le 0 \qquad 0 \le r \le R$$

$$\frac{\partial c}{\partial r} = 0, \qquad r = 0$$

$$D_p \frac{\partial c}{\partial r} = k_f\,(c_b - c), \qquad r = R$$

Solution of Case 2 BDRR Adsorption and Column Adsorption Equations

The solution method used is beyond the scope of this presentation. To summarize we used the numerical method of lines and transformed the PDE's to a set of ODE's and solved the set of ODE's simultaneously. The parameters were estimated from the classical correlations shown and D_m and t are determined as fitting parameters.

Numerical Method

- Method of Lines
  - Transform PDEs to set of ODEs
  - Solve the set of ODEs simultaneously
  - Parameter Estimation

$$D_p = \frac{\varepsilon_p \, \mathrm{D_M}}{\tau} \qquad k_f = J_D \, \frac{u_s}{Sc^{2/3}}$$

$$\mathrm{Re} = \frac{\rho_f \, u_s \, d_p}{\mu_f} \qquad Sc = \frac{\mu_f}{\rho_f \, D_M}$$

- D_M and t are determined as fitting parameters

Adsorption Kinetics for Mercury

The adsorption kinetics for mercury acetate adsorbed on SOL-AD-IV(Thiol) using the BDRR are shown on this slide.[5] The two curves for [Hg] of 5 and 0.5 mg/L for both the chemical reaction and film-pore models essentially overlap.

An average particle diameter of 152 um for the range 125-180 um is used in the calculations. Quantitative evaluation of the two models can be made and the error analysis suggests that the film-pore model better predicts the data.

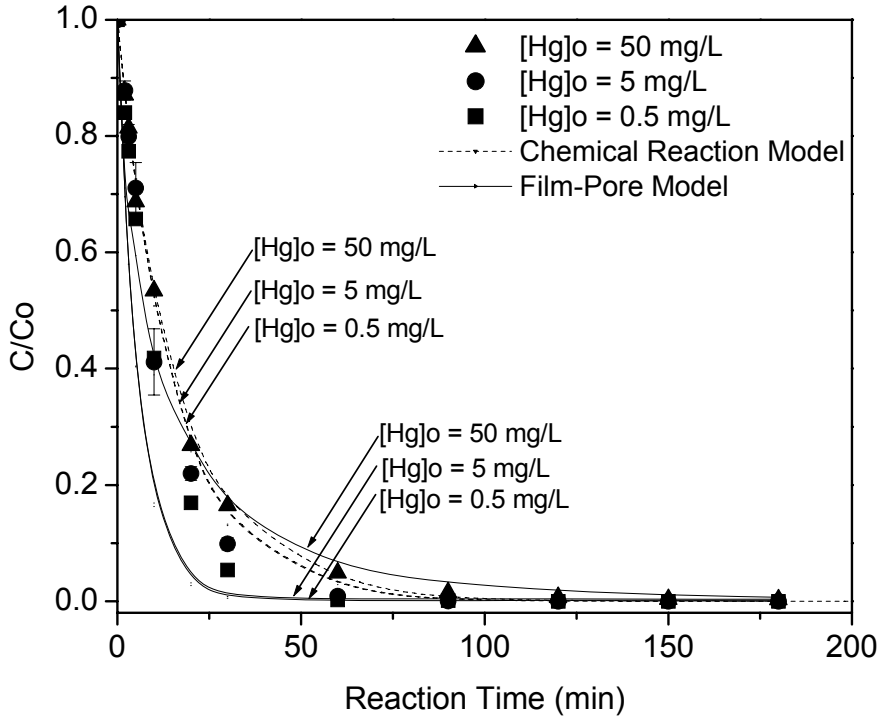

Model	Overall AARD*	D_p (cm^2/s)	k_2 (L/mmol·s)	
Film-Pore	0.35	1.72×10^{-6}	-	**τ = 2**
Chemical Reaction	0.50	-	0.399	

Breakthrough for Mercury

The high mercury concentration [Hg]= 50mg/L breakthrough curve for the experiment and the predicted film-pore differ model is shown in this slide.[5] A good agreement is seen in the comparison.

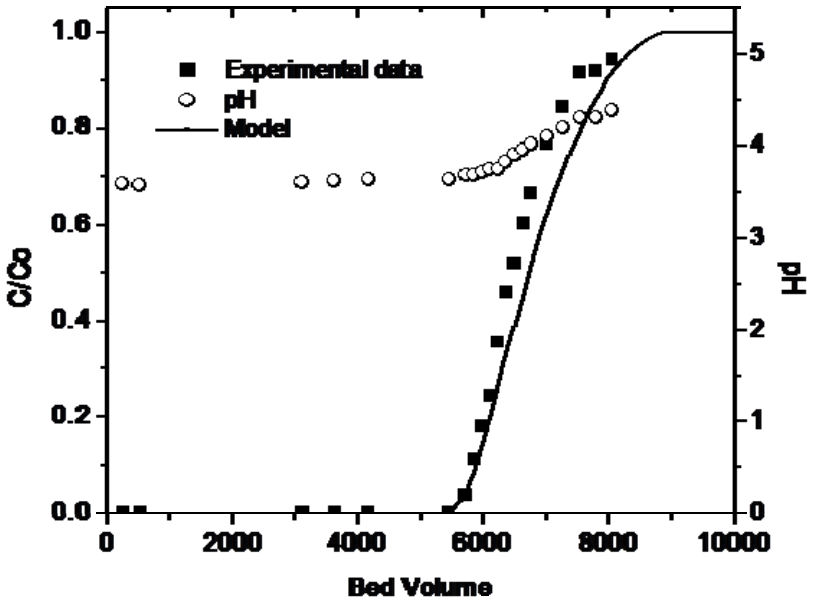

Loading Condition
0.25 mmol/L Hg at pH 5
12 liters into 0.021 liters
0.2 g in 0.7 cm ID column;
Flow rate = 1 ml/min

Adsorption Kinetics for Germanium

Similar adsorption studies in the BDRR are shown in slide 36 to demonstrate utility of this approach for other systems, this case being the adsorption kinetics of germanium. The concentration change of germanium is modeled well at two pH experiments using the film-pore model for the controlling resistance for the adsorption of germanium.[10] The values of the parameters employed and calculations are provided.

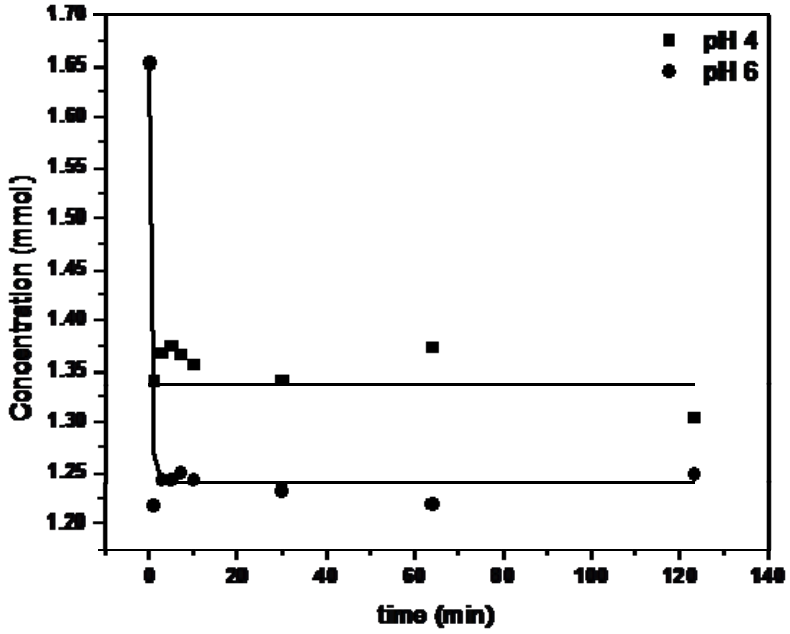

- ini Conc. = 100ppm
- pHe = 4, 6
- Adsorbent = 0.5 g
- Solution volume = 100 ml
- $D_M = 3.8 \times 10^{-6}$ cm^2/s
- $k_f = 1.983 \times 10^{-1}$ cm/s
- $\tau = 0.5$
- $D_p = 2.97 \times 10^{-10}$ m^2/s

Breakthrough for Germanium

Similarly, column breakthrough experiments are modeled using the film-pore model. A good fit of the experimental data is shown in this study as well. The parameters of the experiment are presented and the values for τ and D_p shown in the previous slide were employed.

Also shown is the subsequent stripping experiment. Approximately 90% of the adsorbed germanium can be recovered using the stripping conditions shown.[10]

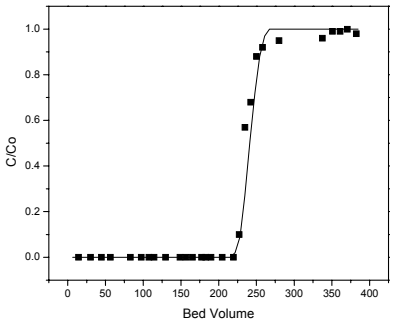

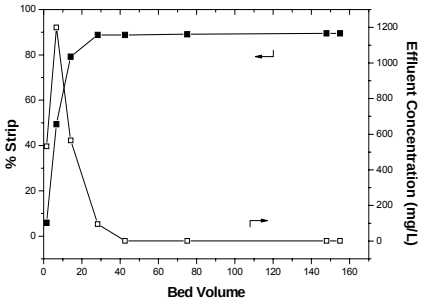

▪Loading Condition

- 0.5 g in 0.7 cm ID Column
- $[Ge]_{in}$ = 51.3ppm
- pH_{in} = 6.11
- Flow rate = 0.86 mL/min
- Capacity = 0.21 mmol/g

▪Stripping Condition

- Strip Conc. = 1M HCl
- Flow rate = 1.08 mL/min
- Stripping Efficiency = 92%

Conclusions

- Examined methods to develop adsorbents through covalent attachment of ligands using sol-gel synthesis techniques.
- Described methods to characterize these adsorbents including ^{29}Si-NMR spectra; uptake capacity studies; BET measurement of pore diameters, porosity and surface area.
- Results show sol-gel adsorbents have metal selectivity, good physical/chemical stability, and capacities comparable to highest polymer resins.
- Three applications were shown for mercury removal, noble metal separations and germanium recovery from zinc leachate solutions. The results are promising.
- Mathematical modeling of batch adsorption was outlined to evaluate the rate determining steps of adsorption when either chemical reaction rate or film-pore diffusion controls.
- Mathematical modeling of fixed bed absorbers was outlined to evaluate breakthrough curves of adsorption columns for the specific separations and sol-gel adsorbents developed.
- The sol-gel systems have potential for application to nuclear fuel separations and the modeling approaches can be employed to design column and evaluate unit operation performance.

Notations

c = metal concentration in the pore, mmol/L
c_b = metal concentration in the bulk, mmol/L
c_{bo} = initial metal concentration in the bulk, mmol/L
c_s = metal concentration at the pellet surface, mmol/L
c_T = total concentration of each metal, mmol/L
D_p = pore diffusion coefficient, cm^2/s
D_M = molecular diffusion coefficient, cm^2/s
K_{eq} = equilibrium constant, $L \cdot g/mmol^2$, L/mmol
k_f = film coefficient, cm/s
q = local concentration in the pellet, mmol of metal/g of adsorbent
q = average concentration in the pellet, mmol of metal/g of adsorbent
r = radial direction of the pellet, cm
R_p = radius of pellet, cm
q_{max} = max capacity of the adsorbent, mmol/g
t = time, min
u_s =superficial velocity, cm/s
V = volume of solution, L
V_R = volume of reactor, L
V_T = volume of tank, L
z = axial direction in the column, cm
τ= particle tortuosity
ε_p = pellet porosity
ε_b = bed porosity
ρ_p = pellet density, g/cm^3
ρ_b = bed density, g/cm^3
ρ_s = solid density of the adsorbent, g/cm^3
θ = corrected time in column calculations, $t-z\varepsilon/u_s$; min, s
k_2 = forward reaction rate constant
k_{-2} = reverse reaction rate constant
M = weight of adsorbent, g
γ = activity coefficient
μ = liquid viscosity, cP

References

1. L. L. Tavlarides; J.S. Lee. New Materials in Solvent Extraction. In Solvent Extraction and Liquid Membranes: Fundamentals and Applications in New Materials (Ion Exchange and Solvent Extraction); Aguilar, M.; Cortina, J. L., Eds.; CRC Press, Florida, 2008; 225-260.
2. N.V. Deorkar; L. L. Tavlarides. Emerging Separation Technologies for Metals II, The Minerals, Metals & Materials Society, Warrendale, Pennsylvania, USA, 1996, 107 – 118.
3. S. S. Gomez; L.L. Tavlarides. Synthesis of thiol functionalized organo-ceramic adsorbent by sol-gel technology, Reactive and Functional Polymers 2001, 49, 159-172.
4. N. V. Deorkar; L. L. Tavlarides. Zinc, Cadmium, and Lead Separation from Aqueous Streams Using Solid-Phase Extractants, Ind. Eng. Chem. Res., 1997, 36, 399-406.
5. K. H. Nam; S. S. Gomez; L. L. Tavlarides. Mercury(II) Adsorption from Wastewaters Using a Thiol Functional Adsorbent, Ind. Eng. Chem. Res. 2003, 42(9), 1955-1964.
6. J. S. Lee; L. L. Tavlarides. Pyrazole Functionalized Organo-Ceramic Hybrids for Noble Metal Separations, AIChE, 2005, 51, 2702-2711.
7. J. S. Lee. MS Thesis, Syracuse University, Syracuse, NY 1997.

8. J. S. Lee; L. L. Tavlarides. Application of Organo-Ceramic Adsorbents Functionalized with Imidazole for Noble Metal Separations, *Solvent Extr. Ion Exch*., 2002, 20(3), 407-427.
9. H. J. Park; L. L. Tavlarides.Adsorption of Chromium (VI) from Aqueous Solution Using an Imidazole Functionalized Adsorbent, *Ind. Eng. Chem. Res*., 2008, 47, 3401-3409.
10. H. J. Park; L. L. Tavlarides. Germanium (IV) Adsorption from Aqueous Solution Using a Kelex-100 Functional Adsorbent, *Ind. Eng. Chem. Res*., 2009, submitted.
11. C. Tien. Adsorption Calculations and Modeling, Butterworth-Heinemann Series in Chemical Engineering, Butterworth Heinemann, Boston, USA, 1994
12. Rovira; J. L. Crotina; J. Arnaldos; A. M. Sastre. Impregnated Resins Containing Di-(2-ethylhexyl) Thiophosphoric Acid for the Extraction of Palladium (II). II. Selective Palladium (II) Recovery from Hydrochloric Acid Solutions, Solvent Extraction and Ion Exchange, 1999, 17, 351-366.
13. M. Iglesias; E. Antico; V. Salvado. Recovery of Palladium (II) and Gold (III) from Dilute Liquors using the Resin Duolite GT-73, Analytica Chimica Acta, 1999, 381, 67-67.
14. A. Sugii; N.. Ogawa; H. Hashizume. Preparation and Properties of Macroreticular Resins Containing Thiazole and Thiazoline Groups, Talanta, 1980, 27, 627-631.
15. X. Feng; G. E. Fryxell; L. Q. Wang; A. Y. Kim; J. Liu; K. M. Kemner. Functionalized Monolayers on Ordered Mesoporous Supports, Science, 1997, 276, 923-926.
16. J. P. Marco; D. Cazorla; S. A. Linares. A New Strategy for Germanium Adsorption on Activated Carbon by Complex Formation. Carbon. 2007, 45(13), 2519-2528.
17. Y. Inukai; Y. Tanaka; Y. Shiraishi; T. Matsuda;, N. Mihara;, K. Yamada; N. Nambu; O. Itho; T. Doi;, Y. Kaida; S. Yasuda. Selective Separation of Germanium (IV) by Di-(2-hydroxyethyl) Amine-Type Cellulose Derivative. Analytical Sciences. 2001, 1, 1117-1120.
18. O. S. Pokrovsky; G.S. Pokrovski; J. Schott; A. Galy. Experimental Study of Germanium Adsorption on Goethite and Germanium Coprecipitation with Iron Hydroxide: X-ray Absorption Fine Structure and Macroscopic Characterization. Geochimica et Cosmochimica Acta. 2006, 70, 3325-3341.
19. M. B. Colella; S. Siggia; R.M. Barnes. Synthesis and characterization of a poly(acrylamidoxime) metal chelating resin. *Anal. Chem.* 1980, 52, 967-9722.